

ATOMIC OXYGEN INTERACTIONS WITH PROTECTED ORGANIC MATERIALS ON THE LONG DURATION EXPOSURE FACILITY (LDEF)

Bruce A. Banks, Kim K. de Groh,
NASA Lewis Research Center
Cleveland, Ohio 44135
Telephone: (216) 433-2308, Fax: (216) 433-2221.

5/3-23

Justine L. Bucholz
Ohio Aerospace Institute
Brook Park, Ohio 44142
Telephone: (216) 433-2308, Fax: (216) 433-2221

171

and

Michael R. Cales
Cleveland State University
Cleveland, Ohio 44115
Telephone: (216) 433-2310, Fax: (216) 433-2221

ABSTRACT

The Long Duration Exposure Facility (LDEF) has provided an excellent opportunity to understand the nature of directed atomic oxygen interactions with protected polymers and composites. Although there were relatively few samples of materials with protective coatings on their external surfaces on LDEF which were exposed to a high atomic oxygen fluence, analysis of such samples has enabled an examination of the shape of atomic oxygen undercut cavities at defect sites in the protective coatings.

Samples of front-surface aluminized (Kapton) polyimide were inspected by scanning electron microscopy to identify and measure crack defects in the aluminum protective coatings. After chemical removal of the aluminum coating, measurements were also made of the width of the oxidized undercut cavities below the crack defects. The LDEF flight undercut cavity geometries were then compared with Monte Carlo computational model undercut cavity predictions.

The comparison of the LDEF results and computational modeling indicates agreement in specific undercut cavity geometries for atomic oxygen reaction probabilities dependent upon the 0.68 to 3.0 power of the energy. However, no single energy dependency was adequate to replicate flight results over a variety of aluminum crack widths.

INTRODUCTION

Atomic oxygen in low Earth orbit readily oxidizes most polymeric materials (1-5).

It is now widely known that the use of unprotected polymeric materials in low Earth orbit may cause unacceptable recession during high atomic oxygen fluence missions. Either new materials should be used which are inherently immune to atomic oxygen attack or conventional materials may continue to be used provided they are covered with atomic oxygen resistant coatings.

Protective coatings for polymers typically used in low Earth orbit, such as SiO_x on polyimide Kapton, have been developed and extensively tested in ground laboratory atomic oxygen systems. However, few high fluence in-space exposure studies of such protected polymers have been conducted (7,8).

On the LDEF spacecraft, relatively few polymers that had metal or metal oxide protective coatings on their exposed surfaces were exposed to high fluence atomic oxygen. A small sample of aluminized (Kapton) polyimide was exposed to high fluence atomic oxygen on LDEF and then used for characterization of the undercut cavities at defect sites in the protective coating. These data were then used for comparison with an *ab initio* Monte Carlo computational model which was developed to predict the shape of the atomic oxygen undercut cavities that occur at defects in protective coatings on polyimide Kapton. The detailed mechanistic assumptions of the computational model could then be varied to examine the degree to which the observed LDEF results matched the model predictions for various mechanistic assumptions.

Understanding the detailed mechanistic interactions which occur between atomic oxygen and protected materials in low Earth orbit will allow more reliable predictions of the long term durability of protected materials in low Earth orbit, based on ground laboratory testing.

METHODS, MATERIALS, AND PROCEDURE

LDEF Aluminized Kapton Samples

A front-surface aluminized (Kapton H) polyimide sample exposed on LDEF as part of the Solar Array - Materials Passive LDEF Experiment located on row 8A was used for the experimental data presented in this investigation. The sample consisted of approximately 1,000 Å of vapor deposited aluminum on a 0.0254 mm thick Kapton substrate. The sample was oriented such that it received a total atomic oxygen fluence of 7.15×10^{21} atoms/cm² arriving at 38.1° from the perpendicular to the surface.

The sample was examined for crack or scratch defects in the aluminization to allow a two-dimensional characterization of the crack width and the associated undercutting. A two-dimensional geometry was desired because the Monte Carlo computational model was also two-dimensional.

Scanning electron microscope photographs were taken of defects with a variety of widths in the aluminized Kapton. The sample was then chemically treated with a dilute hydrochloric acid solution to remove the aluminum. Additional scanning electron micrographs were taken at the identical defect sites to allow measurement of the width of the undercut cavities associated with the defect sites.

The crack-width data, undercut-width data, and undercut-cavity shape were then used as the basis for modeling this behavior with Monte Carlo predicted undercutting geometries based on specific atomic oxygen interaction mechanistic assumptions such as reaction probabilities and fractional energy loss upon impact.

Monte Carlo Computational Model

An *ab initio* Monte Carlo computational model was developed to predict the undercut cavity shape as a result of atomic oxygen interaction with polyimide Kapton at the site of crack defects in the protective aluminum coating. The model allows the atomic oxygen to enter the crack from a fixed direction (as was the case for LDEF), a sweeping direction (as would occur in the case of a solar array surface where the surface rolls with respect to the atomic oxygen arrival direction), or an isotropic arrival direction (as occurs in ground laboratory oxygen plasma exposure tests to simulate low Earth orbital atomic oxygen conditions). For the fixed direction arrival case, the model also allows a thermally distributed arrival direction to be assumed because the atoms are hot ($\approx 1227\text{K}$ for the LDEF mission) (8), which causes transverse velocity variations to occur.

The mathematical model of Kapton underneath the crack defect consisted of an orthogonal array of cells in which the details of the atomic oxygen interaction with each cell were based on mechanisms which were mathematically defined. Figure 1 illustrates the geometry of the Monte Carlo computational model. Figure 2 is a flow chart of the Monte Carlo computational model showing the decision-making process and the iterations used to predict the undercut cavity shape.

The location of atoms being brought into the defect in the aluminum coating is randomly selected. When the atomic oxygen model atom impinges upon the Kapton surface, a random selection is made as to whether or not the oxygen reacts with the Kapton. This selection is based on a prescribed initial impact reaction probability. In general this reaction probability was set at

0.138 (for normal incidence) based on previous experimental and computational investigations (9).

The probability of reaction upon energetic impact was also assumed to be dependent upon the arrival angle, Θ , with respect to the perpendicular to the surface with a $(\cosine \Theta)^{1/2}$ dependence (9,10). The angle-dependent reaction probability was based on the impinging direction with respect to the local surface normal which was based on the average of adjoining Monte Carlo computational model cells.

Oxygen atoms which impinged upon aluminum were treated as if a glass surface was struck where no reaction was possible. However, depending upon the program operator's choice, recombination or ejection and scattering distributions could be prescribed as similar to those used for atomic oxygen ejection from Kapton.

Energy loss upon impact was defined in terms of a fraction of energy loss between the arriving energy and that energy which would be associated with thermally accommodated atomic oxygen. Thus, the atomic oxygen was assumed to be at 4.5 eV upon initial impact and ultimately thermally accommodated down to approximately 0.04 eV after numerous collisions. The atomic oxygen reaction probability was explored for a dependence upon energy proportional to the arriving energy raised to a numerical exponent ranging from 0.68 to 4.

The atomic oxygen which did not react was ejected at an angle which could be selected based on choices made by the Monte Carlo program operator. These choices included elastic scattering, cosine distributed scattering, or a combination of elastic scattering and thermally accommodated cosine distributed emission. One could also select a random probability of recombination of atomic oxygen if it did not react with the Kapton.

The Monte Carlo computational model ray traced each atom until it either reacted with Kapton or exited the undercut cavity. Exiting could be accomplished by leaving through the defect in the aluminum, or, in the case of high fluence exposure, exiting from an aperture produced in the bottom of the Kapton which was not protected.

Undercutting profiles were predicted by the Monte Carlo model and measurements were then made from the undercut profiles produced by the model and compared with actual LDEF data.

The use of the Monte Carlo computational simulation requires a calibration in which actual in-space erosion for a given atomic oxygen fluence is correlated with computational modeling erosion. This is accomplished by using a wide defect in the protective coating to simulate the erosion which would occur in space, using

the Monte Carlo computational model.

The mean depth of erosion for simulated unprotected Kapton was then used to predict the number of atoms, N, required to simulate the actual LDEF in-space damage which would occur at the site of a narrow crack for which experimental data exists from LDEF. Thus the number of atoms required to enter the simulated defect to cause the same damage as would occur during the LDEF mission is given by

$$N = \frac{MEFW}{HDC}$$

where:

M = number of atoms

entering a wide defect for computation simulation calibration

E = in-space erosion yield of polyimide Kapton, cm³/atom

F = atomic oxygen fluence in space for the LDEF coupon, atoms/cm²

W = narrow crack width in Monte Carlo cell units representing the LDEF protective coating cracks

H = wide crack width in units of Monte Carlo cells for simulation of unprotected Kapton for Monte Carlo calibration

D = depth of erosion in units of Monte Carlo cells for the wide defect calibration Monte Carlo simulation

C = Monte Carlo simulation cell edge length, cm/cell.

With the above equation one could then use the Monte Carlo model to predict the atomic oxygen undercutting which would occur in space. The above equation also allows calculation of the scale for the Monte Carlo computational geometry. In the above equation a Kapton in-space erosion yield, E, of 3×10^{-24} cm³/atom was assumed.

RESULTS AND DISCUSSION

The aluminized Kapton sample retrieved from LDEF had cracks which were oriented in such a direction that if one looks down the length of the crack, the average angle of atomic oxygen arrival was 25.9° from the perpendicular to the coated Kapton surface. Figure 3 shows scanning electron micrographs of this sample at a crack defect site in the aluminized coating, before and after removal of the aluminized coating.

As can be seen from Figure 3, the width of undercutting significantly exceeds the width of the crack defect in the aluminized coating.

Figure 4 shows a clear view of the undercut cavity of a similar defect site after removal of the aluminized coating. As can be seen from Figure 4, the undercut cavity is asymmetrical. The left side of the undercut cavity has a chamfer near the top while the right side of the undercut cavity, which does not contain a chamfer, is undercut at such an angle that the cavity wall is not visible in this image. This is thought to be largely due to the fact that incoming atomic oxygen scatters off the edges of the aluminized coating causing the scattered atomic oxygen to preferentially attack the near surface Kapton opposite the side of the defect.

In Figure 4, the atomic oxygen was arriving from the upper left direction. Thus the undercut cavity has rather straight walls on its right side and is more undercut on the left side because of atomic oxygen scattering effects. It was apparent from the micrographs of wide cracks (of the order of $3\mu\text{m}$ on this sample) that the atomic oxygen undercut cavity extended all the way through the 0.0254 mm thick Kapton sample. Narrow cracks in the aluminized layer did not allow sufficient atomic oxygen fluence entry into the undercut cavities to erode all the way through the Kapton, as shown in Figure 5.

Figure 5 also shows the chamfering effects of atomic oxygen reflected from the aluminized coating. The bottom of the undercut cavity is also observable at this rather narrow crack defect site.

Figure 6 shows the results of measurements from the scanning electron micrographs of a variety of crack widths in the aluminized coating and their associated undercut widths, for cracks all oriented in approximately the same direction. This plot, along with the asymmetrical shape of the undercut cavities observed in the scanning electron micrographs, was used as a basis of comparison with Monte Carlo model predictions to assess the validity of mechanistic assumptions for atomic oxygen interaction with polymers and protective coatings.

The Monte Carlo modeling of the LDEF atomic oxygen arrival used the assumptions of reference (8). The angular distribution of atomic oxygen arrival associated with 1227K hyperthermal atoms is shown in Figure 7 as a polar plot of the atomic oxygen arrival flux as a function of the arriving direction.

As can be seen from Figure 7, the arriving atomic oxygen has an angular distribution similar to a searchlight which clearly would indicate that undercut cavities should widen with depth, if a sufficient atomic oxygen fluence has passed through the defect.

Although computational simulations of the LDEF environmental interactions with aluminized Kapton were conducted assuming a variety of atomic oxygen scattering processes (including specular, cosine, and a mix of cosine and specular), only a cosine ejection distribution was found to produce undercut profiles which replicated observed LDEF results.

Figure 8 shows two Monte Carlo predicted undercut cavities. These two predictions were selected for providing reasonable undercut cavity matches to both the undercut shape and the undercut cavity width versus defect width plot of Figure 6. Such models were then developed for reaction probability energy dependent exponents ranging from 0.68 to 3.

As can be seen from Figure 8, atomic oxygen reflected from the aluminized protective coating does produce a slight pocket in the Kapton near the aluminum coated surface as shown in the observed LDEF scanning electron micrographs.

For each reaction probability energy-dependent exponent, a variety of fractional energy losses upon impact were evaluated in an attempt to reproduce the LDEF-observed undercut cavity width versus protective coating defect width data. The results of these efforts are shown in Figure 9. The Monte Carlo predictions are shown as error bars on the figure. The error bars represent the range of undercut widths that could be predicted based on the range of interpretations possible for the width of the undercutting profile. No individual reaction probability energy dependent exponent and its associated fractional energy loss upon impact was found to produce an ideal match to the observed experimental data.

A rather weak energy dependence as shown in Figure 9a produces far too much undercutting for small width defects. Increasing the energy dependence up to an exponent of 3, Figure 9d did produce crack width to undercut width ratios which replicated flight results; however, predicted undercutting for large width cracks was not sufficiently wide to match observed data. Thus, although undercut widths could be predicted which matched LDEF results for specific width cracks, no single energy dependent exponent for reaction probability was found to provide acceptable profile matches over all width cracks. Based on these results further adjustments in the quantification of the mechanistic assumption parameters are necessary.

One of the difficulties associated with performing the Monte Carlo computational calculations is that typically ten hours were needed to produce each predicted Monte Carlo undercutting profile. This is largely a result of Monte Carlo model atoms bouncing around within the undercut defect cavities with a very low reaction probability after they have thermally accommodated. Each atom is required to either react or exit the defect before

another atom is brought into the model cavity. No recombination was assumed to occur in these studies. As the reaction probability decreases with each collision, many impacts are required before the next atom is allowed to enter. Thus, the process of computation slows down greatly as the undercut cavity grows. Although this is an inconvenience, the accuracy of the prediction should not be compromised.

The Monte Carlo model does predict many of the features experimentally observed but will require additional investigation to more clearly quantify the energy dependence and fractional energy loss.

SUMMARY

A retrieved LDEF sample of front surface aluminized Kapton was analyzed by scanning electron microscopy to characterize the atomic oxygen undercut geometries and the dependence of undercut cavity width on the aluminized protective coating crack width.

The undercut cavities observed indicate that atomic oxygen scatters off the edges of the protective coating to produce accentuated atomic oxygen erosion of the Kapton opposite the impinged edge. A Monte Carlo computational model was developed which is capable of simulating a variety of atomic oxygen environments including that of the LDEF spacecraft. This model was used to predict undercut cavity profiles in an attempt to replicate the observed LDEF data.

Although the results of the computational modeling were found to replicate the shape of some of the undercut cavities at defect sites, such replication was not observed over a wide range of crack defect widths. Further study is needed to develop mechanistic information which accurately predicts observed experimental results.

ACKNOWLEDGEMENT

The authors gratefully acknowledge the kind assistance provided by Dr. Ann Whitaker at NASA Marshall Space Flight Center who provided the sample of aluminized Kapton used in this study.

REFERENCES

1. L. J. Leger, "Oxygen Atom Reaction with Shuttle Materials at Orbital Altitudes," NASA TM-58246, 1982.
2. A. F. Whitaker, "LEO Atomic Oxygen Effects on Spacecraft Materials," paper presented at the AIAA Shuttle Environment and Operations Meeting, Washington, D.C., October 31-November 2, 1993, AIAA-83-2632-CP.

3. D. E. Brinza, "Proceedings of the NASA Workshop on Atomic Oxygen Effects," JPL Publication 87-14 (June 1, 1987), Pasadena, CA, Nov. 10-11, 1986.
4. B. A. Banks, M. J. Mirtich, S. K. Rutledge, and D. M. Swec, NASA TM-83706, Paper presented at the 11th International Conference on Metallurgical Coatings sponsored by the American Vacuum Society, San Diego, CA, April 9-13, 1984.
5. W. S. Slemp, D. R. Young, G. W. Witte, Jr., and J. Y. Shen, "Effects of the LDEF Flight Exposure on Selected Polymer Matrix Resin Composite Materials," LDEF-69 Months in Space, First Post-Retrieval Symposium, June 2-8, 1991, NASA CP-3134, Part II, p.1149.
6. B. A. Banks, S. K. Rutledge, K. K. de Groh, M. J. Mirtich, L. Gebauer, R. Olle, and C. M. Till, "The Implications of the LDEF Results on Space Station Freedom Power System Materials," paper presented at the 5th International Symposium on Materials in a Space Environment, Cannes-Mandelieu, France, Sept. 16-20, 1991.
7. S. K. Rutledge, R. M. Olle, and J. M. Cooper, "Atomic Oxygen Effects on SiO_x Coated Kapton for Photovoltaic Arrays in Low Earth Orbit," paper presented at the IEEE/Photovoltaic Specialists Conference, Las Vegas, Nevada, Oct. 7-11, 1991.
8. B. A. Banks, S. K. Rutledge, K. K. de Groh, B. M. Auer, M. J. Mirtich, L. Gebauer, C. M. Hill, and R. F. Lebed, "LDEF Spacecraft, Ground Laboratory and Computational Modeling Implications on Space Station Freedom's Solar Array Materials and Surfaces Durability," paper presented at the IEEE/Photovoltaic Specialists Conference, Las Vegas, Nevada, Oct. 7-11, 1991.
9. B. A. Banks, S. K. Rutledge, K. K. de Groh, C. R. Stidham, L. Gebauer, and C. M. LaMoureaux, "Atomic Oxygen Durability Evaluation of Protected Polymers using Thermal Energy Plasma Systems," paper presented at the International Conference on Plasma Synthesis in Processing of Materials, Denver, Colo., February 21-25, 1993.
10. C. R. Tennyson, G. R. Cool, and D. G. Zimcik, "Space Environmental Effects on Polymer Matrix Composites as a Function of Sample Location on LDEF," paper presented at the LDEF Materials Results for Spacecraft Applications Conference, Huntsville, AL, Oct.27-28, 1992.

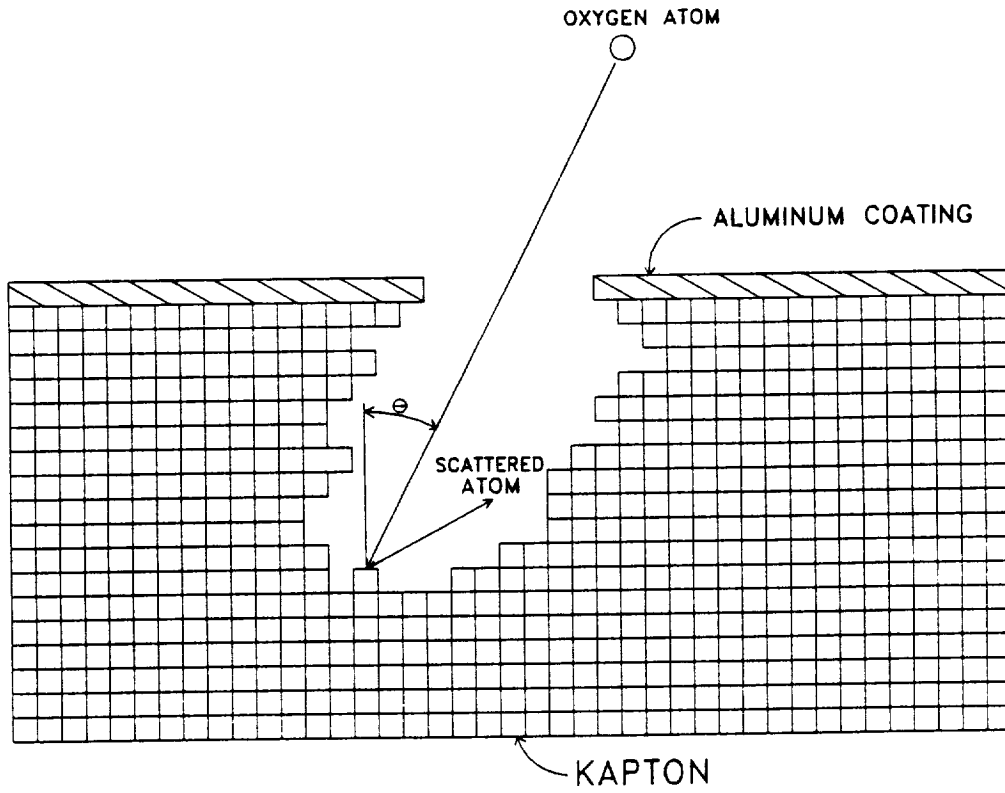


Figure 1. Monte Carlo computational model geometry.

GENERAL OUTLINE

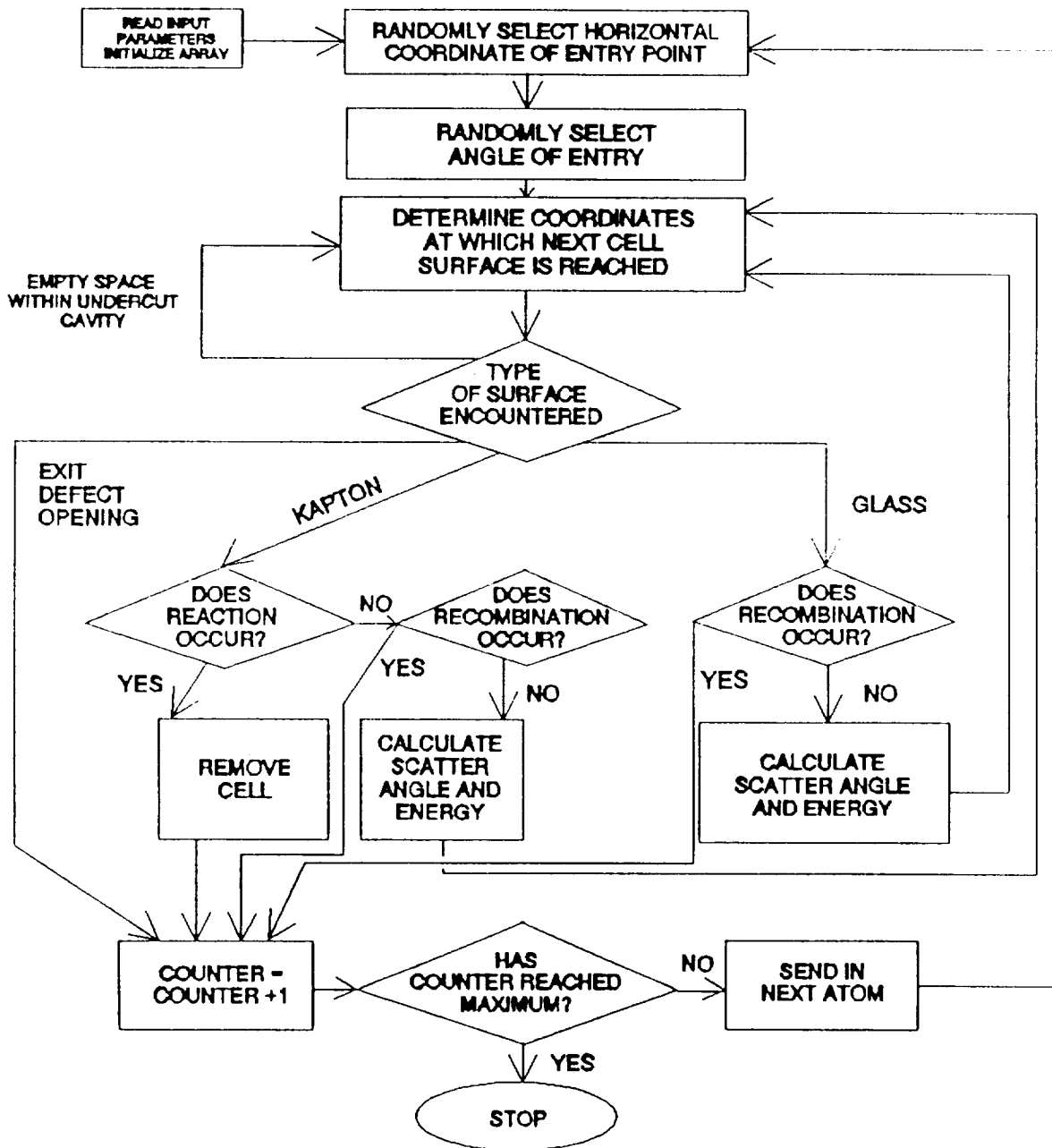
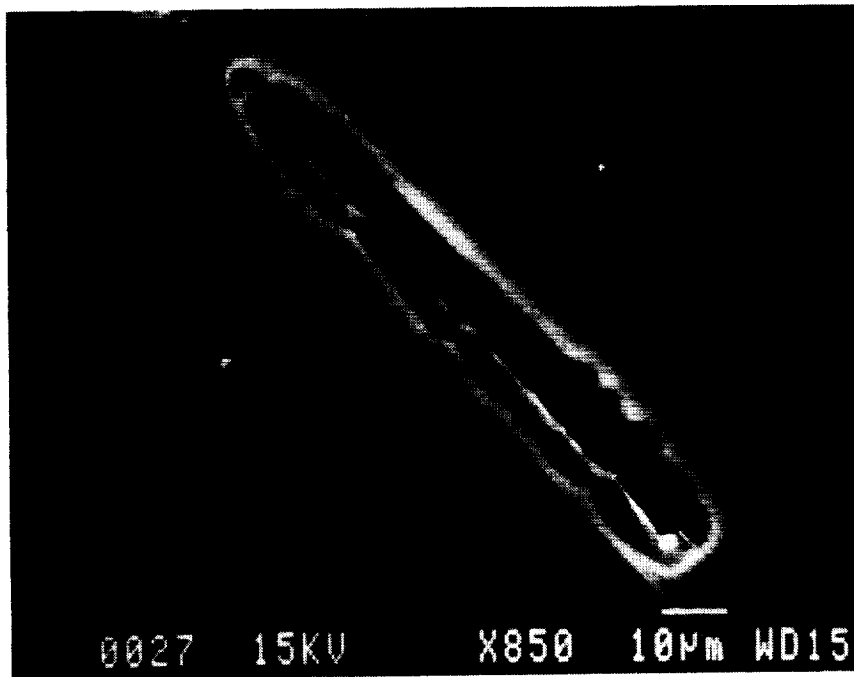
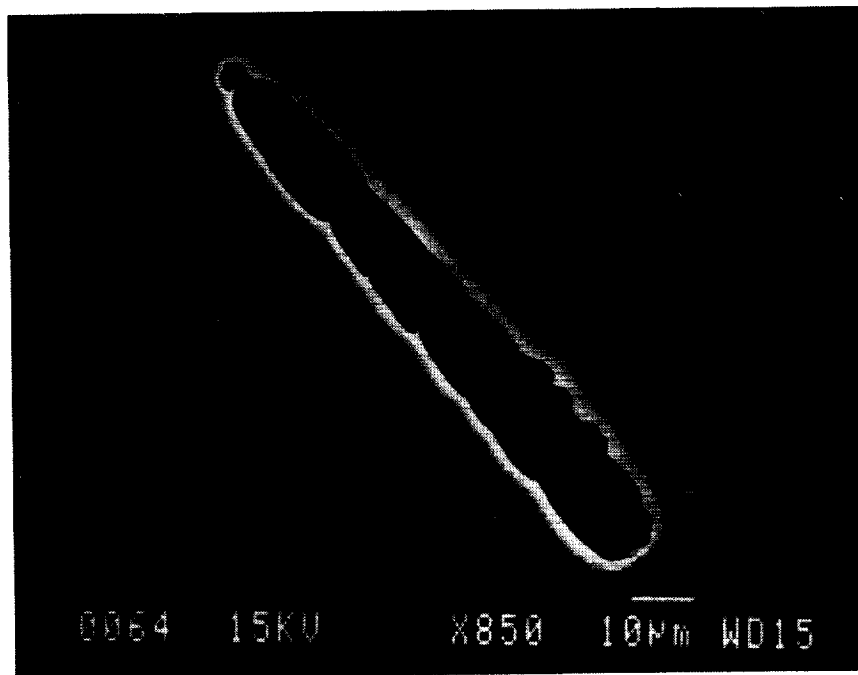


Figure 2. Monte Carlo computational model flow chart.



a. Al coating present



b. Al coating removed

Figure 3. Scanning electron photomicrograph of retrieved LDEF aluminized Kapton sample



Figure 4. Undercut cavity associated with a wide defect in the aluminized Kapton after removal of the aluminized coating.



Figure 5. Undercut cavity beneath a narrow crack in the aluminized coating after removal of the aluminized coating.

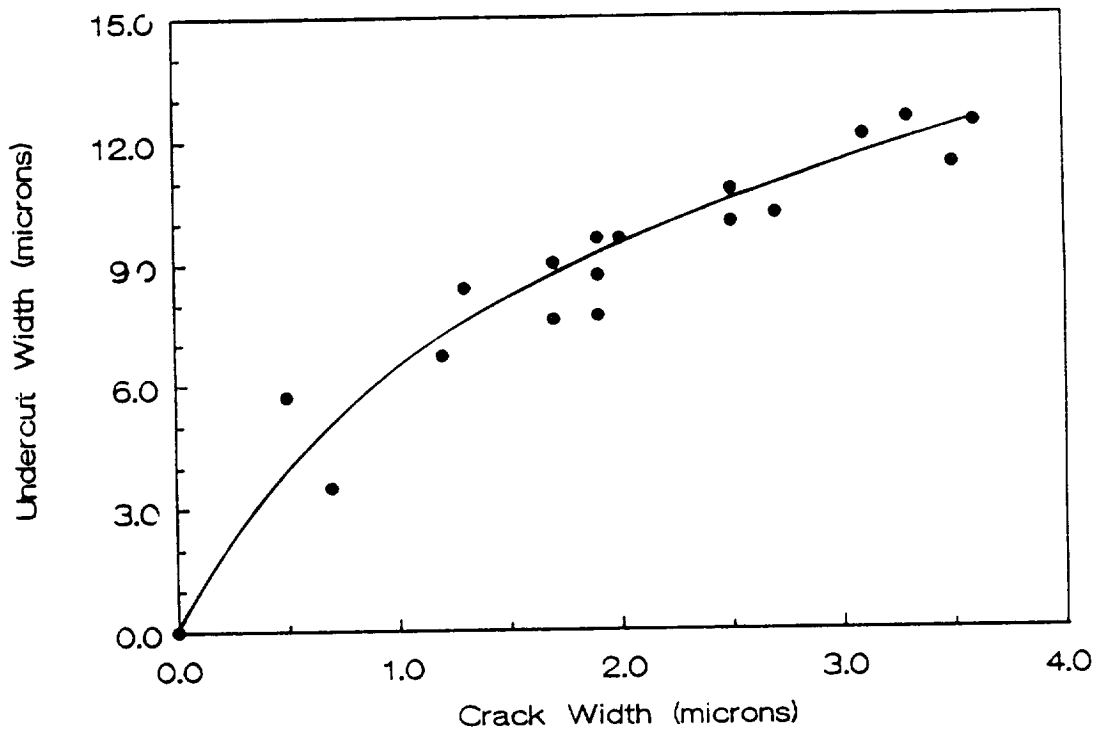


Figure 6. Observed retrieved LDEF sample undercut cavity width dependence upon crack width in the aluminized coating

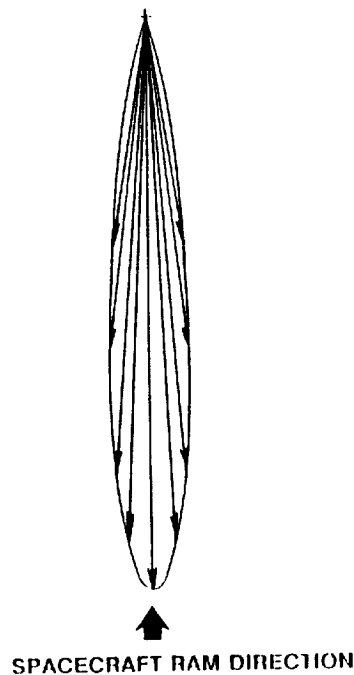
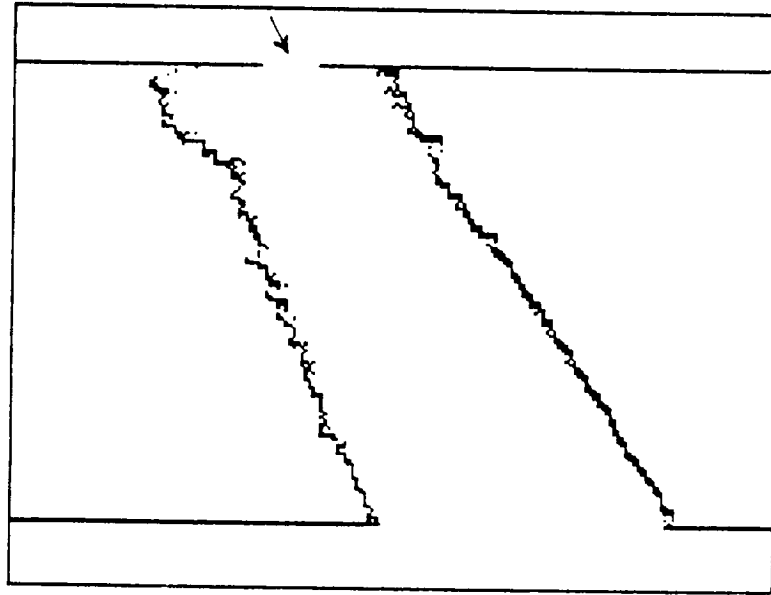
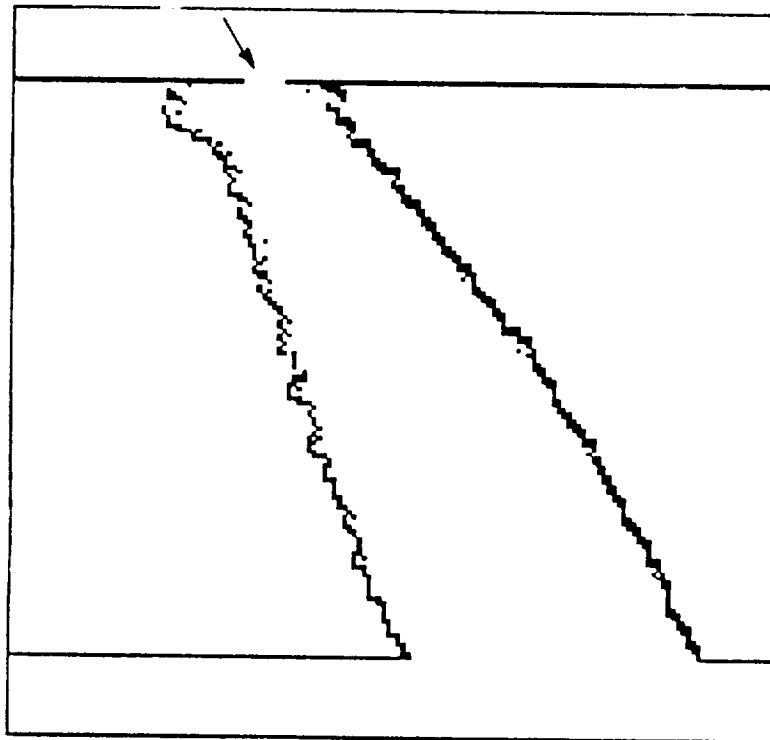


Figure 7. Polar plot of LDEF atomic oxygen arrival resulting from a combination of the spacecraft's orbital velocity, Earth's upper atmosphere co-rotational velocity, the 28.5° inclination of the orbit, and the fact that the spacecraft is ramming into a 1227K gas of atomic oxygen.

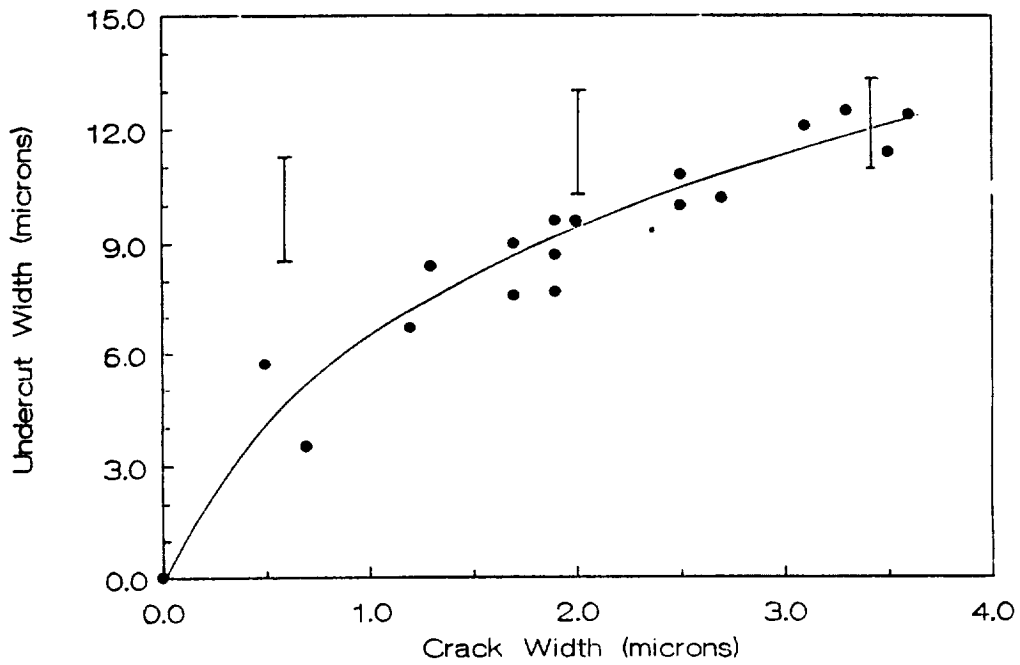


a. 3.4 μm wide crack defect, reaction probability dependent upon $(\text{energy})^{0.68}$, fractional energy loss upon impact equal to 0.4.

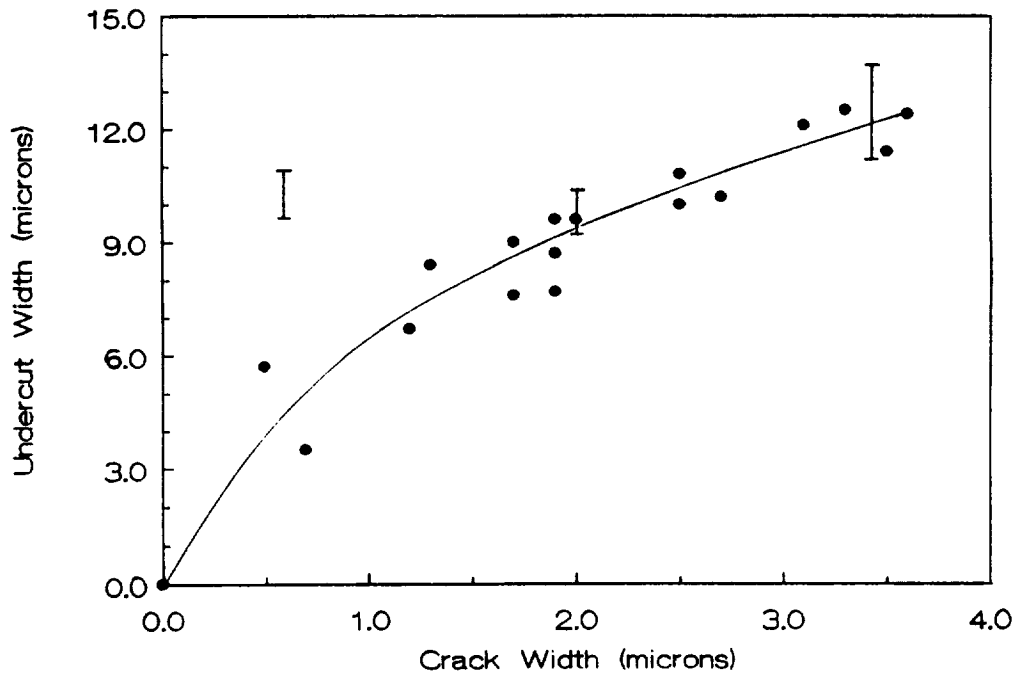


b. 2 μm wide defect in the aluminized coating, reaction probability dependent upon $(\text{energy})^3$, fractional energy loss upon impact equal to 0.2.

Figure 8. Monte Carlo computational model predictions for undercut cavities associated with crack defects in LDEF aluminized Kapton.

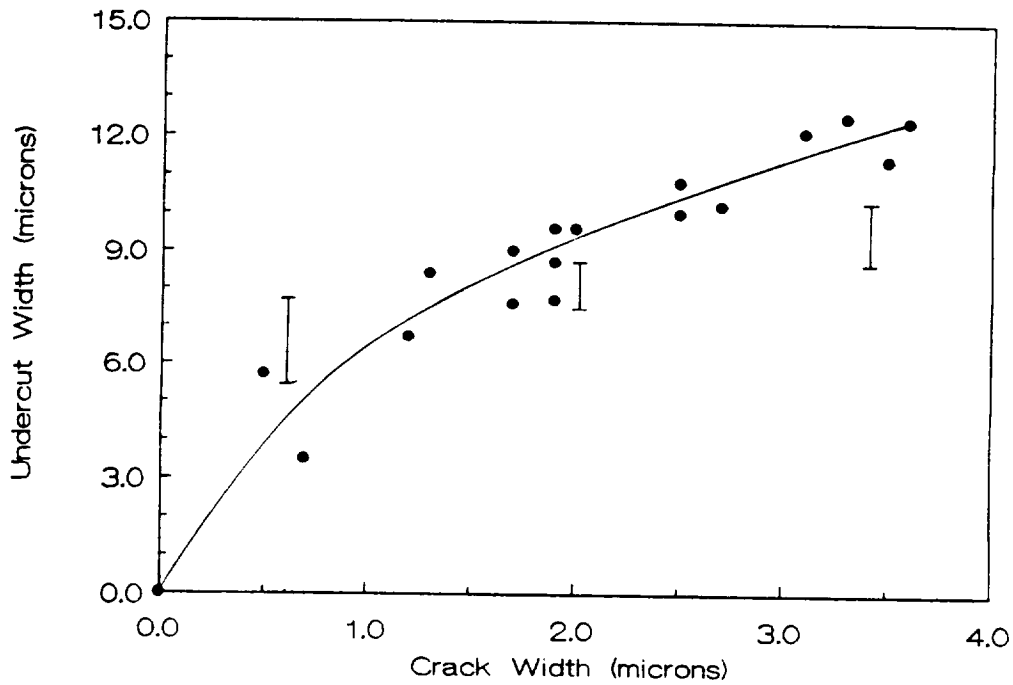


a. Reaction probability proportional to $(\text{energy})^{0.68}$,
fractional energy loss upon impact = 0.4

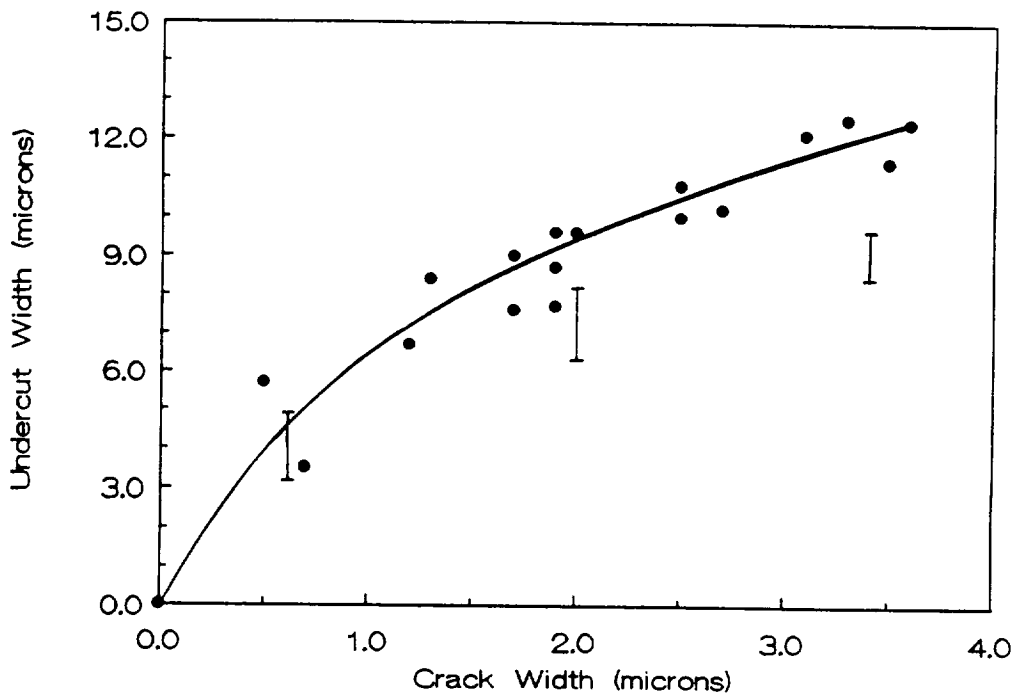


b. Reaction probability proportional to $(\text{energy})^1$,
fractional energy loss upon impact = 0.2

Figure 9. Comparison of Monte Carlo computational model predicted undercutting (shown as error bars) with experimentally observed LDEF data.



c. Reaction probability proportional to $(\text{energy})^2$,
fractional energy loss upon impact = 0.2



d. Reaction probability proportional to $(\text{energy})^3$,
fractional energy loss upon impact = 0.2.

Figure 9. Comparison of Monte Carlo computational model predicted undercutting (shown as error bars) with experimentally observed LDEF data.

